

1 **Historical variation in normalized difference vegetation index**  
2 **compared with soil moisture at a taiga forest ecosystem in**  
3 **northeastern Siberia**

4 Aleksandr Nogovitcyn<sup>1</sup>, Ruslan Shakhmatov<sup>1,2</sup>, Tomoki Morozumi<sup>3</sup>, Shunsuke Tei<sup>4,5</sup>, Yumiko  
5 Miyamoto<sup>4,6</sup>, Nagai Shin<sup>7</sup>, Trofim C. Maximov<sup>8</sup> and Atsuko Sugimoto<sup>4</sup>

6 <sup>1</sup>Graduate School of Environmental Science, Hokkaido University, Sapporo, 060-0817, Japan

7 <sup>2</sup>Slavic-Eurasian Research Center, Hokkaido University, Sapporo, 060-0809, Japan

8 <sup>3</sup>National Institute for Environmental Studies, Tsukuba, 305-8506, Japan

9 <sup>4</sup>Arctic Research Center, Hokkaido University, Sapporo, 001-0021, Japan

10 <sup>5</sup>Forestry and Forest Products Research Institute, Tsukuba, 305-8687, Japan

11 <sup>6</sup>Faculty of Agriculture, Shinshu University, Kamiina, 399-4598, Japan

12 <sup>7</sup>Research Institute for Global Change, Japan Agency for Marine-Earth Science and Technology, Yokohama, 236-0001, Japan

13 <sup>8</sup>Institute for Biological Problems of Cryolithozone, Siberian Branch of the Russian Academy of Sciences, Yakutsk, 677000,  
14 Russia

15 *Correspondence to:* Atsuko Sugimoto (sugimoto@star.dti2.ne.jp)

16 **Abstract.** The taiga ecosystem in northeastern Siberia, a nitrogen-limited ecosystem on permafrost with a dry climate,  
17 changed during the extreme wet event in 2007. We investigated the normalized difference vegetation index (NDVI) as a  
18 satellite-derived proxy of needle production and compared it with ecosystem parameters such as soil moisture water  
19 equivalent (SWE), larch foliar C/N ratio,  $\delta^{13}\text{C}$  and  $\delta^{15}\text{N}$ , and ring width index (RWI) at the Spasskaya Pad Experimental  
20 Forest Station in Russia for the period from 1999 to 2019. Historical variations in NDVI showed a large difference between  
21 typical larch forest (unaffected) and the sites affected by the extreme wet event in 2007 because of high tree mortality at  
22 affected sites under extremely high SWE and waterlogging, resulting in a decrease in NDVI, although there was no  
23 difference in the NDVI between typical larch forest and affected sites before the wet event. Before 2007, the NDVI in a  
24 typical larch forest showed a positive correlation with SWE and a negative correlation with foliar C/N. These results indicate  
25 that not only the water availability (high SWE) in the previous summer and current June but also the soil N availability likely  
26 increased needle production. NDVI was also positively correlated with RWI, resulting from similar factors controlling them.  
27 However, after the wet event, NDVI was negatively correlated with SWE, while NDVI showed a negative correlation with  
28 foliar C/N. These results indicate that after the wet event, high soil moisture availability decreased needle production, which  
29 may have resulted from lower N availability. Foliar  $\delta^{15}\text{N}$  was positively correlated with NDVI before 2007, but after the wet  
30 event, foliar  $\delta^{15}\text{N}$  decreased. This result suggests damage to roots and/or changes in soil N dynamics due to extremely high  
31 soil moisture. As a dry forest ecosystem, taiga in northeastern Siberia is affected not only by temperature-induced drought but  
32 also by high soil moisture, led by extreme wet events, and nitrogen dynamics.

33 **1 Introduction**

34 Boreal forests in northern regions of North America and Eurasia, including islands, occupy a large area, approximately 27 %  
35 of the world's forest cover (FAO, 2020). Under conditions of increasing atmospheric CO<sub>2</sub> concentrations (e.g. Friedlingstein  
36 et al., 2022), the role of taiga and other terrestrial ecosystems as carbon sinks becomes more important. Among the taiga  
37 areas, Alaska, Canada, and Siberia are distinguished by permafrost, which is one of the main components of the global  
38 carbon cycle. Under warming conditions, northern ecosystems respond differently to environmental changes depending on  
39 the different biomes and regions, as mentioned below from remote sensing satellite observations. The normalized difference  
40 vegetation index (NDVI), the most common remote sensing vegetation data, typically shows increasing trends (greening) in  
41 arctic tundra but decreasing trends (browning) in many boreal forests (Bunn and Goetz, 2006; Verbyla, 2008; Berner and  
42 Goetz, 2022; Miles and Esau, 2016). Observed greening at the tundra and taiga-tundra boundary can be associated with the  
43 expansion of trees and shrubs to the north (Frost and Epstein, 2014; Tape et al., 2006; Shevtsova et al., 2020) and increases in  
44 aboveground plant biomass (Goetz et al., 2005; Berner et al., 2013; Forbes et al., 2010). In turn, the browning of taiga can be  
45 attributed to tree mortality and decreases in forest production because of droughts (Welp et al., 2007; Bunn and Goetz, 2006),  
46 forest fires (Goetz et al., 2005), and extreme wet events (Famiglietti et al., 2021; Nogovitcyn et al., 2022). Nevertheless,  
47 temporal changes in the NDVI of boreal forests are spatially heterogeneous and vary depending on different factors, such as  
48 the plant vegetation types (Myers-Smith et al., 2020; Bunn and Goetz, 2006), stand density (Bunn et al., 2007; Dearborn and  
49 Baltzer, 2021) and topography (Sato and Kobayashi, 2018). One of the most important factors controlling greenness is water  
50 availability (Ruiz-Perez and Vico, 2020; Forkel et al., 2015). Overall, warming condition of boreal forests has positive effects  
51 in wetter regions but negative effects on forest productivity in dry regions (e.g., Ruiz-Perez and Vico, 2020).

52 Siberian taiga is mainly covered with deciduous conifers, larches, which grow under severe conditions, such as continental  
53 climate, that is, cold winters, hot summers, low precipitation (Archibald, 1995), and limited nitrogen availability (Popova et  
54 al., 2013; Kajimoto et al., 1999). Permafrost and seasonal ice are important sources of water for larches during drought  
55 (Sugimoto et al., 2003; Sugimoto et al., 2002). These severe conditions make this ecosystem vulnerable to environmental  
56 changes. In northeastern Siberia, the role of the taiga ecosystem and its responses to climate change have been studied at the  
57 Spasskaya Pad Forest Station near Yakutsk over a long-term. Over the past few decades, the ring width index (RWI) has  
58 decreased in this region as well as in other continental dry regions, Alaska, Canada, and southern Europe, because of high  
59 temperature-induced droughts (Tei et al., 2017). On the other hand, precipitation extremes, which are predicted to be more  
60 intensive and frequent (Douville et al., 2021; Wang et al., 2021), can also negatively affect the forest. In addition to droughts,  
61 extreme wet events occur because of intensive precipitation, such as heavy rainfall and snowfall. In this forest area, changes  
62 in winter precipitation may shift the forest phenology and production of soil inorganic nitrogen, as demonstrated in snow  
63 manipulation experiments (Shakhmatov et al., 2022).

64 In northeastern Siberia, boreal forests have been affected by drought in the past because of the continental climate. However,  
65 in 2007, soil moisture was the highest in the past century (Tei et al., 2013) because of large amounts of rainfall and  
66 subsequent winter snowfall, which led to waterlogging in topographic depressions of the forest. This extreme wet event was  
67 fatal for many trees in the forest, especially in the depressions (Iijima et al., 2014; Ohta et al., 2014). These extremely moist  
68 conditions reduced CO<sub>2</sub> uptake by vegetation (gross primary production) and evapotranspiration (Ohta et al., 2014).  
69 Evapotranspiration in this region is mainly controlled by the leaf area index (LAI) (Matsumoto et al., 2008), suggesting a  
70 decrease in LAI in 2007 because of high tree mortality. However, after the extreme wet event, eddy-covariance flux  
71 measurements showed no significant trends in CO<sub>2</sub> exchange at the ecosystem scale (Kotani et al., 2019). The affected sites  
72 are distinguished not only by high tree mortality but also by a secondary succession of the understory and floor vegetation  
73 communities to water-resistant species, which may have compensated for the reduced water and CO<sub>2</sub> fluxes (Ohta et al.,  
74 2014).

75 Boreal forests in northeastern Siberia have been affected by both drought and extreme wet events, as described above, which  
76 involved complex changes in the forest environment. Tei et al. (2019a) demonstrated that larch trees, which died during the  
77 extreme wet event, were affected by a previous drought. However, at the forest level, the NDVI was not related to gross  
78 primary production in 2004–2014 (Tei et al., 2019b), and the NDVI of the larch forest damaged by waterlogging showed  
79 insignificant trends in 2000–2019 and an insignificant correlation with climate data (Nagano et al., 2022). These phenomena  
80 were attributed to waterlogging-induced changes in the understory and floor vegetation composition (Nagano et al., 2022; Tei  
81 et al., 2019b), but they seem to be also related to changes in the conditions of the larch forest.

82 The taiga ecosystem in eastern Siberia is one of the most important biomes in the world and is vulnerable to climate change.  
83 The purpose of this study was to understand how the larch forest in this region changed, particularly after the extreme wet  
84 event in 2007, and what factors impacted the changes over the past two decades. Therefore, we investigated historical  
85 variations in satellite-derived NDVI to evaluate changes in the forest, as the leaves of deciduous trees reflect the condition of  
86 trees in each year. To understand the factors impacting forest changes, especially related to the extreme wet event, NDVI data  
87 were compared with field-observed parameters in a typical larch forest, such as the RWI, soil moisture, needle δ<sup>13</sup>C, δ<sup>15</sup>N,  
88 C/N, air temperature, and precipitation from 1998 to 2019.

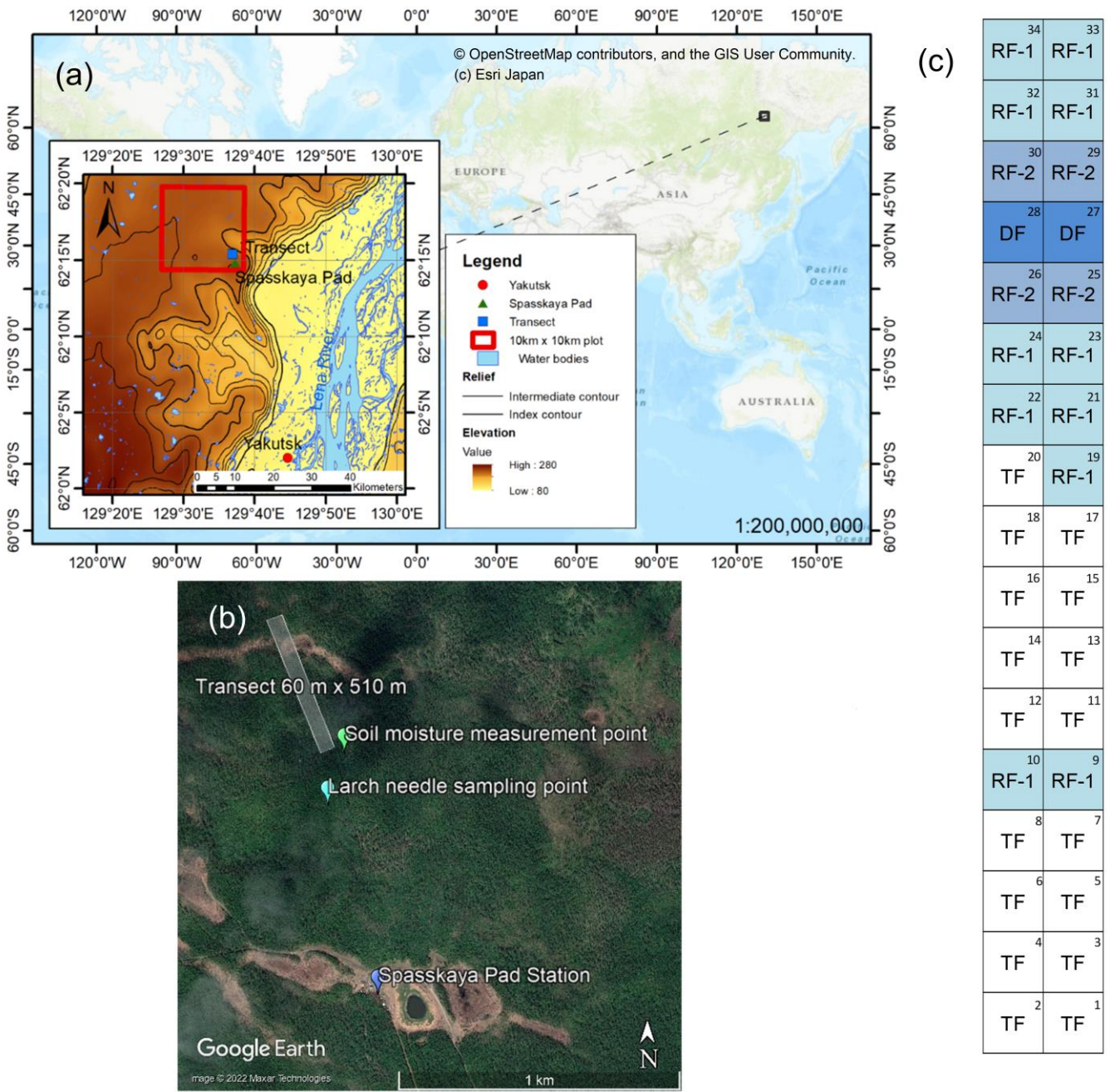
## 89 **2 Materials and Methods**

### 90 **2.1 Study site**

91 The study was conducted in the Spasskaya Pad Experimental Forest (62°15'18"N, 129°37'08"E, alt. 220 m a.s.l.), Institute  
92 of Biological Problems of Cryolithozone, Siberian Branch of the Russian Academy of Sciences (IBPC SB RAS), near  
93 Yakutsk, Russia (Fig. 1a). The region in Eastern Siberia is established on continuous permafrost and has a continental climate

94 (dry climate) with an extremely high annual temperature range. During the observation period from 1991 to 2020 at Yakutsk,  
95 the average annual precipitation was 233 mm, and the average monthly temperature ranged from -37°C to +20 °C in cold  
96 January and warm July, respectively. Dominant species is larch (*Larix cajanderi*) that is deciduous conifer (Abaimov et al.,  
97 1998), mixed with broadleaved birch (*Betula pendula*), and the understory includes small shrubs, such as evergreen cowberry  
98 (*Vaccinium vitis-idaea*) and deciduous bearberry (*Arctous alpina*), and grasses.

99 During the period from 2005 to 2007 (water years, from October to September), there was a large amount of precipitation  
100 ( $307 \pm 29$  mm) continuously, which caused a significant increase in soil moisture (Sugimoto, 2019) and even waterlogging.  
101 Consequently, an extreme wet event occurred in 2007, which damaged larch forests, resulting in high tree mortality and a  
102 change in the composition of understory vegetation to moisture-tolerant grasses and shrubs in some areas, especially in  
103 depressions (Iijima et al., 2014; Iwasaki et al., 2010; Ohta et al., 2014). In the summer of 2018, we set a 60 m  $\times$  510 m  
104 transect, which included areas unaffected and affected by the extreme wet event (Fig. 1a, b). The transect was divided into 30  
105  $\times$  30 m plots (34 plots in total). Using these plots, we observed spatial variation in NDVI (Nogovitcyn et al., 2022). In this  
106 study, we visually classified the forest conditions based on photographs. Four forest types were identified along the transect  
107 (Fig. 1c): typical mature (TF; number of plots in the transect,  $n = 17$ ), regenerating-1 (RF-1;  $n = 11$ ), regenerating-2 (RF-2;  $n$   
108 = 4), and damaged (DF;  $n = 2$ ) forests. The first TF showed no visible damage from the extreme wet event. The plots  
109 discerned as regenerating forests RF-1, had many dead mature larches and formed forest gaps in the overstory where there  
110 were a large number of young larches (seedlings and saplings with a height of up to 3 m) and shrubs. Regenerating forests,  
111 RF-2, contained more dead mature larches and more young larches compared to those in RF-1. Damaged forests, DF, where  
112 all mature trees died, was predominantly covered by moisture-tolerant grasses, and had much smaller numbers of young  
113 larches than in RF-1 and RF-2. The DF plots were located on a depression in a trough-and-mound topography, and some  
114 patches of the DF plots were flooded.



115

116 **Figure 1.** (a) Location of the Spasskaya Pad Station (62°15'18"N, 129°37'08"E) and the study transect near Yakutsk in the topographic  
 117 map (modified from USGS/NASA Landsat 8 image) zoomed from a global map (Source: © OpenStreetMap contributors, © Esri Japan).  
 118 (b) Detailed view of the study area in the Spasskaya Pad Forest (Source: © Google Earth, © 2022 Maxar Technologies): locations of the  
 119 station, 60 m x 510 m transect, and points of soil moisture measurement and larch needle sampling for  $\delta^{13}\text{C}$ ,  $\delta^{15}\text{N}$ , and C/N. (c) Scheme of  
 120 the transect with a total of 34 plots, which were divided into four forest types based on the level of forest damage (Nogovitcyn et al., 2022):  
 121 typical forests (TF), two types of regenerating forests (RF-1 and RF-2), and damaged forests (DF).

## 122 2.2 NDVI

123 The raster normalized difference vegetation index (NDVI) was computed based on the Landsat Collection-1 Level-2 image  
 124 products (<https://earthexplorer.usgs.gov/>) with a spatial resolution of 30 m using QGIS software (v. 3.2.2-Bonn):

$$\text{NDVI} = (\text{NIR} - \text{R}) / (\text{NIR} + \text{R}),$$

where NIR and R are the near-infrared and red surface reflectance bands of the product, respectively. The image products georeferenced to the WGS-84 UTM 52N coordinate system were selected according to the location of the study transect. The NDVI value was extracted for each transect plot using the zonal statistics function. The transect plots, which consist of only pixels attributed to quality pixels (clear terrain, low-confidence cloud, and low-confidence cirrus) in the quality assessment bit index band according to Landsat Surface Reflectance product guides, were used in the analysis.

To investigate the historical variation in NDVI, we considered the seasonal maximum of the mean NDVI of the transect for the long-time period from 1999 to 2019. The longest time-series data available for the study area has been obtained by the Landsat 7 satellite with the Enhanced Thematic Mapper Plus (ETM+) image sensor since 1999. However, its sparse temporal resolution (16 days) and scan-line corrector failure in 2003 forced the consideration of additional data from other satellites, such as Landsat 5 Thematic Mapper (TM) (available until 2011) and Landsat 8 Operational Land Imager (OLI) (available since 2013). Because the last two have different sensors in contrast to Landsat 7, NDVI values calculated from the TM and OLI images were converted to ETM+ using the linear equations:

$$\text{NDVI}_{\text{ETM}+} = 1.037 \cdot \text{NDVI}_{\text{TM}},$$

$$\text{NDVI}_{\text{ETM}+} = 0.9589 \cdot \text{NDVI}_{\text{OLI}} + 0.0029$$

developed by Ju and Masek (2016) and Roy et al. (2016), respectively, for boreal forests. Local parametrization of signals from different sensors was not performed for our study site because of the insufficient overlap in the acquired images. We identified that the selected and converted data were close to the 1:1 lines between Landsat 5 and 7 and between Landsat 7 and 8. For each year, a paired sample *t*-test was applied to determine the difference between the mean NDVI of the transect on the observation days. In the case of statistically insignificant differences among observation days, we selected the day with the highest number of quality pixels.

To verify the historical variation in NDVI of the transect, a larger area, 10 km × 10 km (hereafter, the 10-km plot), including the Spasskaya Pad Forest, was used for comparison with the transect (the center of the 10-km plot was located at 62°17'4"N, 129°32'4"E; Fig. 1a). For each observation day, the mean NDVI of the 10-km plot was calculated using only quality pixels using ENVI 5.1 (L3Harris Technologies, USA). For each year, the seasonal maximum NDVI of the 10-km plot was determined as the highest mean NDVI among observation days, on which the number of quality pixels were more than 50 % (total, 111,556 pixels). The seasonal maximums of the transect and 10-km plot showed the same day for about three-quarters of the study period (15 years among 21) and showed a different day in six years (Table S1): 2006 (7 August and 29 July), 2007 (1 and 25 July), 2010 (1 and 15 July), 2011 (5 and 12 August), 2015 (23 and 31 July), and 2019 (1 and 9 July). The averaged NDVI values of the 10-km plot, transect, and each forest type (TF, RF-1, RF-2, and DF) in the transect are shown in Fig. 2a and 2b.

156 The NDVI data of larch forest, which is deciduous, quickly increases in early summer, when the NDVI is mostly stable (e.g.,  
157 Huete et al., 2002). This stable NDVI continues for more than 1.5 months (typically from July to mid-August), although the  
158 time period depends on the weather and soil moisture conditions. Seasonal maximum NDVI was identified during this  
159 period. Although the data acquisition days were limited because of the low temporal resolution and cloud coverage, more  
160 than three days of data were acquired by combining three satellite images, and seasonal maximums were determined, except  
161 for in 1999 and 2003. These two years had only one data acquisition day, on 27 August 1999 and 21 July 2003, and both data  
162 points were recognized as the seasonal maximum.

### 163 **2.3 Ecosystem and climate parameters**

164 Several ecosystem parameters have been observed since 1998 in typical forests. To monitor the physiological response of  
165 larch to environmental changes, the C and N isotopic compositions ( $\delta^{13}\text{C}$  and  $\delta^{15}\text{N}$ , ‰), and the ratio of C to N content (C/N)  
166 of larch needles have been observed since 1999, except in 2012, at the site 200 m south of the transect (Fig. 1b). The  $\delta^{13}\text{C}$   
167 and  $\delta^{15}\text{N}$  are calculated by:

$$168 \quad \delta^{13}\text{C} \text{ (or } \delta^{15}\text{N}) = (R_{\text{sample}}/R_{\text{std}} - 1) \times 1000 \text{ (‰)},$$

169 where  $R_{\text{sample}}$  and  $R_{\text{std}}$  are isotope ratios ( $^{13}\text{C}/^{12}\text{C}$  or  $^{15}\text{N}/^{14}\text{N}$ ) of the sample and standard, respectively, and standards are  
170 Vienna PeeDee Belemnite for C and atmospheric  $\text{N}_2$  for N. The foliar  $\delta^{13}\text{C}$  reflects the physiological condition of  
171 photosynthesis and is widely applied to indicate plant water use efficiency (Farquhar et al., 1989). The  $\delta^{13}\text{C}$  value of plant  
172 tissue (e.g., leaf) is expressed using the following equation:

$$173 \quad \delta^{13}\text{C} = \delta^{13}\text{C}_{\text{atm}} - a - (b - a) (C_i/C_a),$$

174 where  $\delta^{13}\text{C}_{\text{atm}}$  is the C isotopic composition of atmospheric  $\text{CO}_2$ , a (4.4‰) and b (27‰) are isotope fractionations of the  
175 diffusion and photosynthetic reaction, and  $C_i$  and  $C_a$  are intercellular and atmospheric  $\text{CO}_2$  concentrations. The foliar  $\delta^{13}\text{C}$   
176 becomes high when higher irradiance and lower stomatal conductance are observed. At our study site, lower and higher  $\delta^{13}\text{C}$   
177 values of larch needles were typically due to wet and drought conditions. The foliar  $\delta^{15}\text{N}$  is a physiological indicator of the N  
178 source for a plant (Evans, 2001), which can vary depending on numerous physiological and environmental factors. The foliar  
179 C/N represents the N status of a plant (Liu et al., 2005).

180 Larch needles were collected from four to eight young larch trees in August every year. We collected them from the same  
181 trees (sample trees) every August, and these trees are located nearby to each other. Four stems were obtained from each tree,  
182 and the needles from each tree were mixed and analyzed at Kyoto University (samples for 1999–2003) and Hokkaido  
183 University (samples after 2004) using Conflo systems (EA 1108 and Delta S, and Flash EA 1112 and Delta V, Thermo Fisher  
184 Scientific, at Kyoto and Hokkaido Universities, respectively). Analytical precisions (standard deviation) of the C and N  
185 content measurements were better than 0.3% and 0.1%, respectively, and those for the isotopic compositions  $\delta^{13}\text{C}$  and  $\delta^{15}\text{N}$   
186 were better than 0.2‰. The details of sampling, sample preparation and laboratory analyses of C and N contents and their

187 isotope compositions using the EA-IRMS system are described in Fig. S1. The details of the average calculations are shown  
188 in Fig. S1 and S2. In 2015, there were no data on the  $\delta^{15}\text{N}$  and N content.

189 For more than 100 years, until 2016, larch ring-width index (RWI) indicating wood growth dynamics was estimated by  
190 detrending and standardizing the raw time-series width data obtained from the collected paired cores (Tei et al., 2019b; Fan et  
191 al., 2021). The RWI data used for analysis are shown in Table S2.

192 Soil moisture was measured using time-domain reflectometry (TDR), and the soil moisture water equivalent (SWE; the  
193 amount of liquid water contained within the soil layer, mm) in the 0–60 cm soil layer was obtained for 1998–2019 in June,  
194 July, and August using the method described by Sugimoto et al. (2003) (near the transect; Fig. 1b). There were no data for  
195 June of 2002 and 2011 and August of 2003. The details of the intra- and inter-annual variations in SWE are shown in Fig. S3.  
196 Among the climate variables, summer air temperature and precipitation datasets recorded by the meteorological station at  
197 Yakutsk (62.02° N, 129.72° E) were obtained from the All-Russia Research Institute of Hydrometeorological Information -  
198 World Data Centre (RIHMI-WDC) website (<http://aisori-m.meteo.ru/>).

## 199 **2.4 Statistical analysis**

200 All statistical analyses were carried out using R statistics v.4.1.3 (R Core Team). Relationships between datasets were  
201 investigated using a simple linear regression model (function “lm”) and a Pearson correlation test (“cor.test”), the most  
202 common statistical test based on the method of covariance. Trends of NDVI change in 1999–2019 were estimated using the  
203 Mann–Kendall test (package “trend”, function “mk.test”). Differences in NDVI among four forest types (TF, RF-1, RF-2 and  
204 DF) were determined using Kruskal-Wallis test (“kruskal.test”) with pairwise Wilcoxon rank sum test  
205 (“pairwise.wilcox.test”). The results of the statistical tests are shown in the Supplemental (Table S3–S9). The models and  
206 tests described by levels of statistical significance (*p*-values) less than 0.05 and 0.1 were considered to be “significant” and  
207 “moderately significant”, respectively.

## 208 **3 Results**

### 209 **3.1 Year-to-year variation of seasonal maximum NDVI**

210 Fig. 2a shows the historical variation in the seasonal maximum NDVI of the TF and the 10-km plot from 1999 to 2019. Both  
211 NDVI time series varied similarly. The seasonal maximum of each year was observed from 25 June to 13 August, except for  
212 1999 (shown in Table S1). The maximum transect NDVI in 1999 was observed on 27 August ( $0.75 \pm 0.02$ ,  $n = 34$ ) because  
213 the Landsat data in 1999 were limited to the latter half of August. The mean seasonal maximum NDVI for the transect varied  
214 between 0.72 and 0.80. During the period from 1999 to 2001, the NDVI of the transect was high from  $0.75 \pm 0.02$  ( $n = 34$ ) to  
215  $0.80 \pm 0.02$  ( $n = 34$ ) (Fig. 2a), but in 2002 and 2003, the NDVI was much lower ( $0.73 \pm 0.02$ ,  $n = 34$ ) than that in 2001. From

216 2003 to 2006, NDVI again increased from  $0.73 \pm 0.02$  ( $n = 34$ ) to  $0.76 \pm 0.02$  ( $n = 34$ ). During the wet event in 2007–2008,  
217 the NDVI decreased to  $0.73 \pm 0.04$  ( $n = 34$ ). After 2009, NDVI was higher than that in 2008 ( $0.72 \pm 0.03$ ,  $n = 34$ ), except in  
218 2016 ( $0.72 \pm 0.03$ ,  $n = 31$ ).

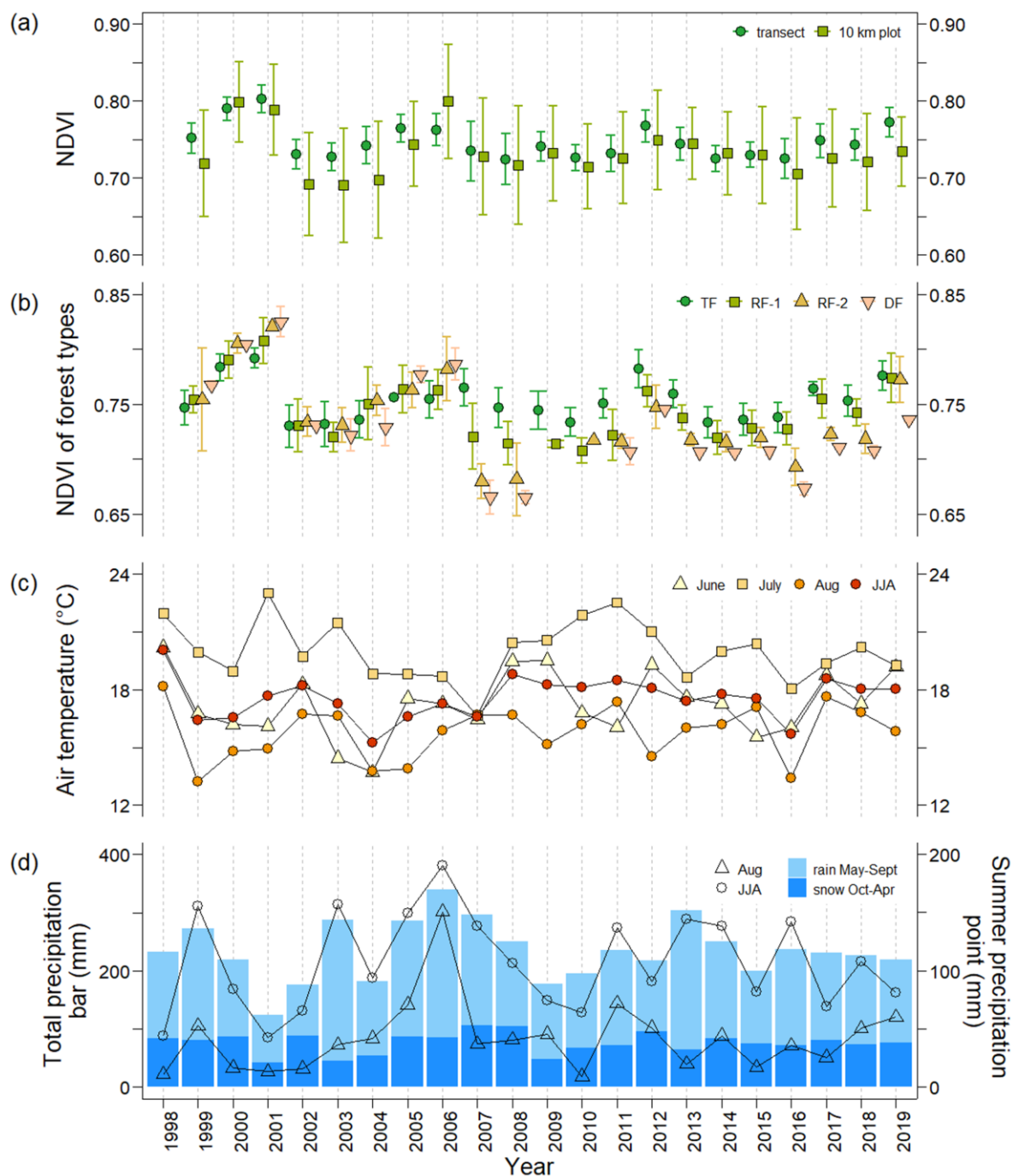


**Figure 2.** The temporal variations from 1999 to 2019 in (a) seasonal maximum NDVI averaged for the plots in the transect and the representative 10-km forest plot calculated from available Landsat 5, 7, 8 images; (b) NDVI of four forest types, typical mature forest (TF), regenerating forests (RF-1 and RF-2), and damaged forest (DF); (c) mean air temperature in June, July, August and whole summer period JJA (June-July-August); (d) the amount of precipitation during previous October-current April (snow) and current May-September (rain) shown with blue bars, in August and whole summer period JJA (June-July-August) shown with triangles and circles. Both the mean NDVI of the 10-km plot and the transect decreased from 1999 to 2019 (-0.0009 and -0.0010 year<sup>-1</sup>, respectively), but not with statistically significant trends. Generally, the mean NDVI in the transect was higher than that in the 10-km plot, except for 2000 and 2014.

228 **3.2 NDVI of each forest type**

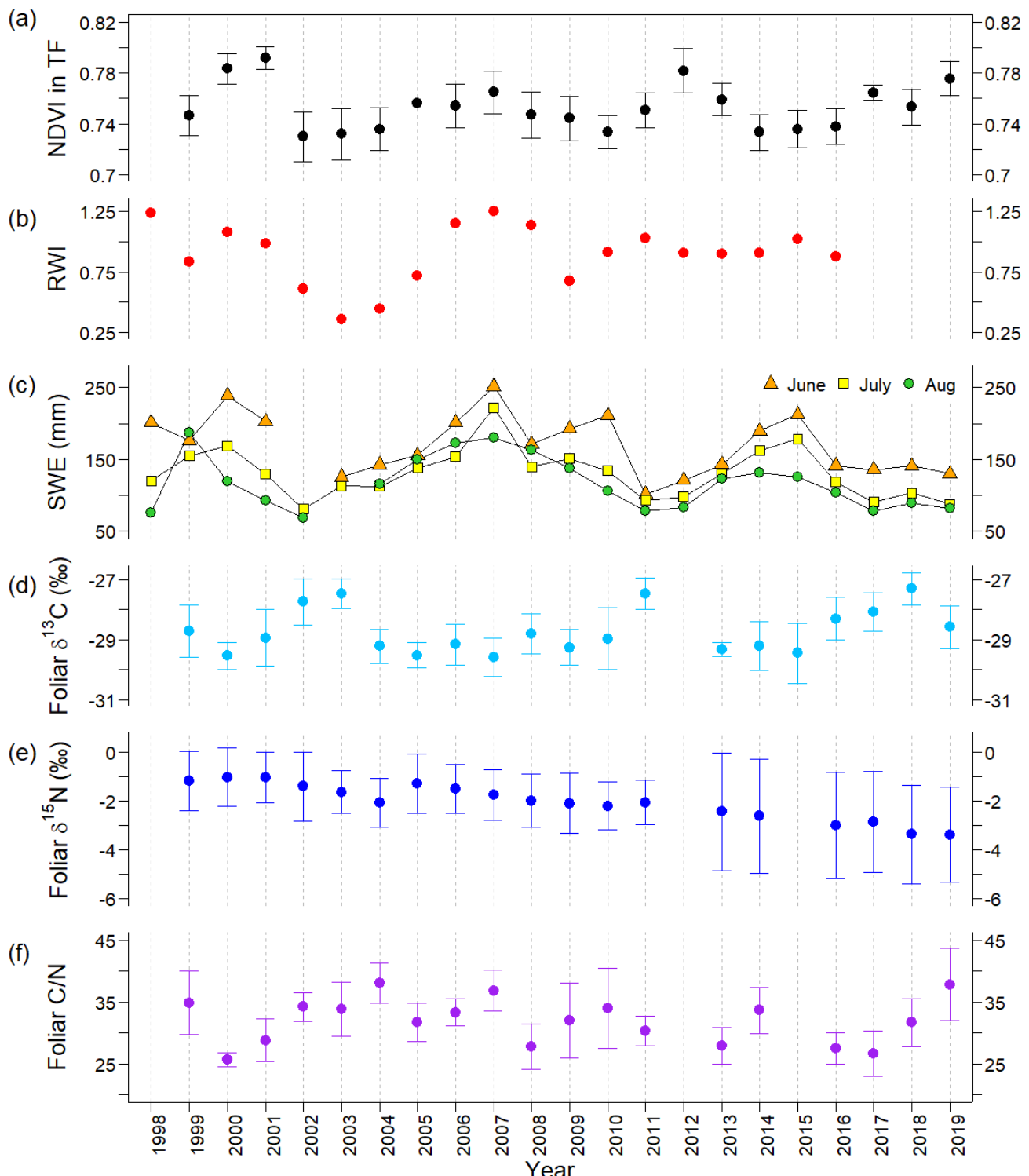
229 The NDVI time series for four forest types (typical forest TF, regenerating forests RF-1 and RF-2, and damaged forest DF) in  
230 the transect during 1999–2019 are shown in Fig. 2b. As shown in Fig. 2b and 3a, before 2007, the NDVI of TF during 1999–  
231 2001 ( $0.75 \pm 0.02$  to  $0.79 \pm 0.01$ ,  $n = 17$ ) was higher than that in the subsequent period, 2002–2006 ( $0.73 \pm 0.02$  to  $0.75 \pm$   
232  $0.02$ ,  $n = 17$ ). In 2002, there was a significant decrease in the TF NDVI, which remained low between 2002 and 2004 (Fig.  
233 2b and 3a). During 1999–2006, the NDVI values of the four types were close to each other, but after the wet event, NDVI  
234 values noticeably differed among the forest types (Fig. 2b). In 2007, the NDVI of TF ( $0.76 \pm 0.02$ ,  $n = 17$ ) was the highest,  
235 and those of the other three types decreased in the order of RF-1 ( $0.72 \pm 0.03$ ,  $n = 11$ ), RF-2 ( $0.68 \pm 0.02$ ,  $n = 4$ ), and DF  
236 ( $0.67 \pm 0.02$ ,  $n = 2$ ) (Fig. 2b). In 2008, the NDVI decreased slightly and showed the same order of forest types as that in  
237 2007. After 2009, the difference among the forest types, especially between TF and DF, remained, although it was smaller  
238 than that in 2007.

239 **3.3 NDVI of the typical forest and ecosystem parameters of the study site**

240 To consider the historical variation in the NDVI of typical forests in our study area, the TF NDVI and observed parameters  
241 were compared (Fig. 2 and 3). In Fig. 4, the linear relationships between NDVI and other parameters were investigated for  
242 two different time periods, before (1999–2006) and after (2008–2019), to compare them.

243 **3.3.1 Climate parameters (temperature and precipitation) at Yakutsk**

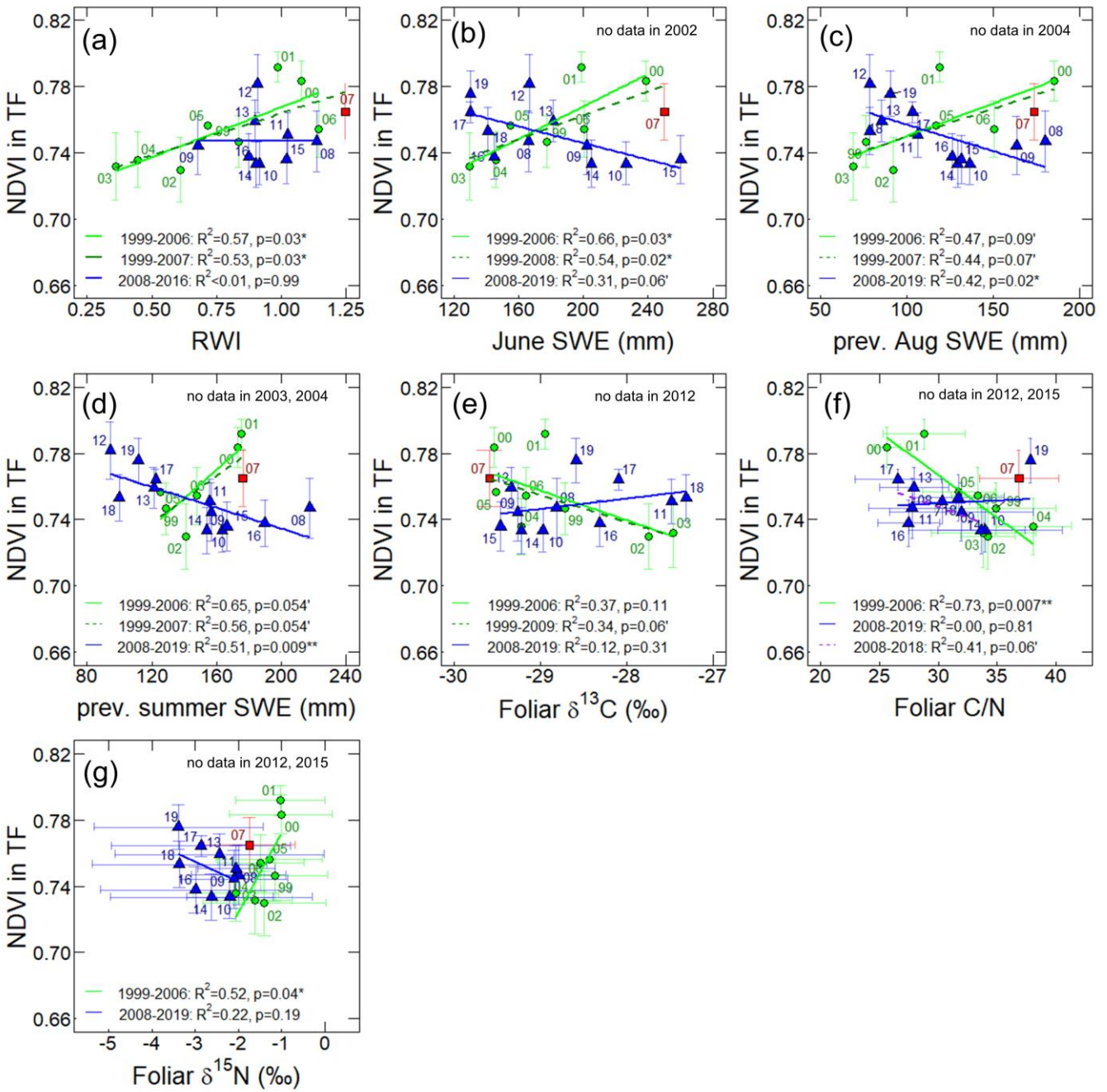
244 Interannual variations in climatic parameters, such as air temperature and precipitation, from 1999 to 2019 are displayed in  
245 Fig. 2c and 2d. The average air temperature in June–August (summer temperature) was relatively high in 1998, 2001–2002,  
246 and 2008–2012 (Fig. 2c). The TF NDVI showed no correlation with summer temperature. The amount of annual water  
247 precipitation (from October to September) for the period from 1991 to 2020 averaged approximately  $233 \pm 47$  mm. As shown  
248 in Fig. 2d, larger water year precipitation, that is, precipitation higher than 280 mm (one standard deviation above the mean  
249 for 1991–2020), was observed in 2003 (287 mm), 2005–2007 (285, 340, and 296 mm), and 2013 (304 mm). The amount of  
250 water precipitation in 2001 (124 mm) was the lowest during the observation period. The drought year (2001) showed a high  
251 TF NDVI value. Consecutive wet years in 2005–2007 showed slightly higher TF NDVI values, but there was no correlation  
252 between the water year precipitation and NDVI.



253

254

Figure 3. The temporal variations in ecosystem parameters observed during 1998–2019 at the typical forest (TF): (a) NDVI, (b) larch ring width index (RWI), (c) soil moisture water equivalent (SWE) at the depth of 0–60 cm in June, July, and August, (d) average foliar  $\delta^{13}\text{C}$ , (e)  $\delta^{15}\text{N}$ , and (f) C/N ratio. Error bars represent standard deviations. There were no data for NDVI in 1998, RWI during 2017–2019, June SWE in 2002, August SWE in 2003, foliar  $\delta^{13}\text{C}$  in 1998 and 2012, and foliar  $\delta^{15}\text{N}$  and C/N in 1998, 2012, and 2015.



258

259 **Figure 4.** The relationships between the TF NDVI in transect and (a) larch RWI during 1999–2016, the monthly average of SWE (mm) in  
260 (b) June and (c) the previous August, (d) averaged monthly SWE for June–August of the previous year, (e) foliar  $\delta^{13}\text{C}$ , (f) C/N, and (g)  
261  $\delta^{15}\text{N}$  during 1999–2019. The green circles, red square, and blue triangles show data points during 1999–2006, 2007, and 2008–2019,  
262 respectively. Labels nearby the data points are observation years of the TF NDVI. Horizontal and vertical error bars represent standard  
263 deviations. Green and blue solid lines show linear regressions for 1999–2006 (before the wet event) and 2008–2019 (after the wet event),  
264 respectively, and dark green and purple dotted lines represent other periods.  $p$ -values and  $R^2$  describe the significance and coefficient of  
265 determination of the regression models, respectively.

### 266 3.3.2 RWI at the typical forest

267 The larch RWI showed a trend similar to that of the transect TF NDVI during 1999–2007 (Fig. 3a and b). The RWI and

268 average TF NDVI showed high values in 2000–2001 (0.98–1.08 and 0.78–0.79) followed by low values in 2002–2003 (0.36–  
269 0.61 and 0.73); the RWI in 2003 was the lowest for the whole observation period. Subsequently, both parameters increased  
270 by 2007 (1.25 and 0.76). After 2007, these two parameters exhibited different behaviors. During the period from 2010 to  
271 2013, a one-year time lag was observed in the TF NDVI: there was an increase in RWI from 2009 to 2011, a decrease in  
272 2012, and one year later, from 2010 to 2012, the TF NDVI increased and then decreased in 2013. Statistically, the temporal  
273 correlation between the TF NDVI and RWI was positive at a significant level during 1999–2016 ( $r = 0.47, p < 0.05$ ; Table  
274 S7), with a stronger significant positive correlation before 2007 ( $r = 0.76, p < 0.05$ ; Fig. 4a, Table S5) and an insignificant  
275 negative correlation after 2007 (Fig. 4a, Table S6).

### 276 3.3.3 Soil moisture water equivalent at the typical forest

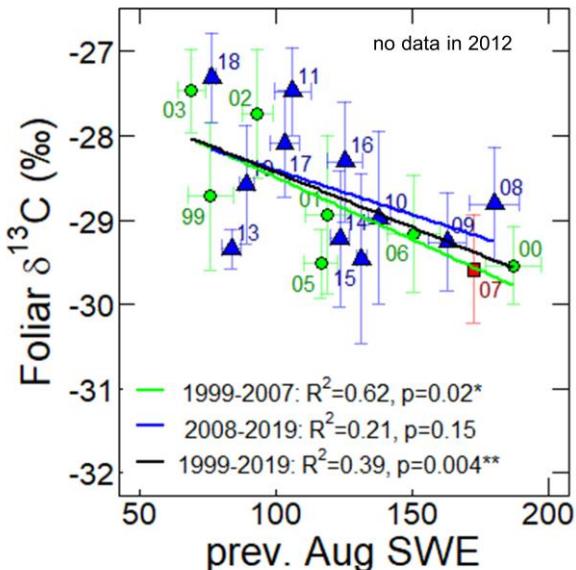
277 The time series of the SWE and TF NDVI showed different correlations in the early and late halves of the observation period  
278 (Fig. 3a and 3c). During 1999–2007, the averaged SWE for June–August (hereafter, summer SWE) and the TF NDVI mostly  
279 showed similar trends. High values of the TF NDVI in 2000 and 2001 corresponded to high values of the SWE in the current  
280 June (239 and 202 mm) and in the last summer (173 and 176 mm in 1999 and 2000). These high values of TF NDVI and  
281 SWE were followed by low values during the drought period in 2002–2003. Subsequently, as summer SWE increased from  
282 2004 (124 mm) to 2007 (218 mm), the TF NDVI also increased. For the period from 2008 to 2019, the correlation between  
283 the TF NDVI and summer SWE was negative, with a one-year time lag in the SWE (Fig. 3a and 3c). A low summer SWE  
284 value was observed in 2011 (91 mm), and a high TF NDVI value was observed in the subsequent year, 2012. After 2016, the  
285 TF NDVI showed an increasing trend, whereas the SWE decreased from 2015 to 2019. Statistically, the TF NDVI showed  
286 positive correlations with the SWE in the current June ( $r = 0.83, p < 0.05$ ) and the previous summer ( $r = 0.79, p < 0.1$ ),  
287 including the previous July ( $r = 0.82, p < 0.05$ ) and previous August ( $r = 0.69, p < 0.1$ ), during the period from 1999 to 2006  
288 (Fig. 4b–d and S4d; Table S5). However, after 2008, TF NDVI showed negative correlations with the SWE in the previous ( $r$   
289 = -0.65,  $p < 0.05$ ) and current ( $r = -0.73, p < 0.01$ ) summer, at a stronger significance level (Fig. 4b–d and S4a–e; Table S6).  
290 During and after 2007, there was no change in the TF NDVI; slightly damaged RF-1 showed a decrease in NDVI to levels  
291 similar to those observed during the 2002 drought (Fig. 2b).

292 3.3.4 Larch needle  $\delta^{13}\text{C}$ ,  $\delta^{15}\text{N}$ , C/N at the typical forest

293 As shown in Fig. 3a and 3d, the foliar  $\delta^{13}\text{C}$  and TF NDVI moved in opposite directions in the early half of the observation  
 294 period (from 1999 to 2009) (Fig. 3a and 3d). For example, in 2000 and 2001, the TF NDVI had large values, while the foliar  
 295  $\delta^{13}\text{C}$  values were low ( $-29.5 \pm 0.5$  and  $-28.9 \pm 0.9\text{‰}$ ). During the period from 2002 to 2007, TF NDVI increased, and at the  
 296 same time, foliar  $\delta^{13}\text{C}$  values decreased. Foliar  $\delta^{13}\text{C}$  values higher than  $-28.0\text{‰}$  were observed in 2002, 2003, 2011, and  
 297 2018, when low summer SWE and TF NDVI were observed (Fig. 3a and 3d). The correlation between foliar  $\delta^{13}\text{C}$  and TF  
 298 NDVI was statistically insignificant without a time lag (Fig. 3e, Tables S5–7), but there was a significant correlation between  
 299 foliar  $\delta^{13}\text{C}$  and TF NDVI with a one-year time lag of foliar  $\delta^{13}\text{C}$  after the wet event (Table S6). Foliar  $\delta^{13}\text{C}$  was negatively  
 300 correlated with the previous August SWE during 1999–2007 ( $r = -0.79, p < 0.05$ ) and 1999–2019 ( $r = -0.62, p < 0.01$  (Fig.  
 301 5), but also with the SWE in the current year June and July for the period from 1999 to 2007, and June to August for 2008 to  
 302 2019 (Table S8).

303 Similar to  $\delta^{13}\text{C}$ , foliar C/N and TF NDVI moved in opposite directions (Fig. 3a and 3f). In 2000 and 2001, the foliar C/N had  
 304 low values ( $25.6 \pm 1.1$  and  $28.8 \pm 3.4$ , respectively), while the TF NDVI was high. There was also a distinct negative  
 305 correlation between trends in C/N and TF NDVI before and after 2007, excluding 2019 (Fig. 4f).

306 Foliar  $\delta^{15}\text{N}$  values decreased after 2005 (Figure 3e). A positive correlation was observed between foliar  $\delta^{15}\text{N}$  and TF NDVI  
 307 before 2007 (Fig. 3a, 3f, and 4g).



308

309 **Figure 5.** The relationship between the foliar  $\delta^{13}\text{C}$  and monthly mean SWE in the previous August (mm) during 1999–2019. The green  
 310 circles, red square, and blue triangles show data points during 1999–2006, 2007, and 2008–2019, respectively. Labels nearby the data  
 311 points are observation years of the foliar  $\delta^{13}\text{C}$ . Vertical error bars represent standard deviations. The linear regressions for 1999–2007,  
 312 2008–2019, and 1999–2019 are presented by green, blue, and black solid lines.  $p$ -values and  $R^2$  describe the significance and coefficient of  
 313 determination of the regression models, respectively.

## 315 4.1 NDVI variation among forest conditions

316 Before 2007, there was a small difference in the NDVI among the four forest types (Fig. 2b and Table S3 and S4). In some  
 317 years before 2007, the NDVI values in RF and DF were higher than those in TF. The difference in elevation between the  
 318 south and north ends of the transect (approximately 5 m according to Google Earth) may lead to differences in soil moisture;  
 319 therefore, the RF and DF plots showed higher soil moisture contents and a lower possibility of drought compared with TF  
 320 before 2007. During 2007–2008, there was a large difference in NDVI among the forest types, especially between the TF and  
 321 DF (Fig. 2a). During this period, the SWE reached extremely high values (Fig. 3c), caused by a large precipitation amount  
 322 during 2005–2008 (Fig. 2d). Consequently, the forest floor was partially waterlogged, resulting in damage to the larch forest,  
 323 especially in the DF and RF plots. These data indicate that during the drought years (before 2007), wet sites such as DF and  
 324 RF showed higher NDVI values than dry TF sites because of higher water availability. However, after 2007, the TF, which  
 325 was visually unaffected by the wet event, showed a higher NDVI than the DF and RF. The presence of surface water in DF  
 326 and soil saturated with water in DF and RF could also reduce the NDVI values. Water predominantly absorbs NIR radiation  
 327 and therefore has a low NIR reflectance, resulting in a lower NDVI than that of vegetation (Holben, 1986).

328 After 2009, as the soil became dry, the difference in NDVI among the forest types decreased (Fig. 2b). This may have been  
 329 caused by the change in the vegetation in RF and DF, that is, the change from mature larch trees to understory and floor  
 330 vegetation, such as water-tolerant species and seedlings of birch and larch trees via secondary succession. In 2016, the  
 331 difference in NDVI between TF and DF increased again (Fig. 2b). This may have been caused by the high SWE observed in  
 332 2015 (Fig. 3c), which lowered the NDVI in RF and DF.

333 However, the difference in NDVI between TF and DF remained at the end of the observation period. Previously, the spatial  
 334 variation in NDVI along the transect was investigated a decade after the wet event in 2018 (Nogovitcyn et al., 2022).  
 335 Nogovitcyn et al. (2022) concluded that NDVI was higher in TF than in DF because of a difference in the stand density of  
 336 mature trees, as NDVI indicates a leaf area index (LAI), which corresponds to the number of mature trees in this forest.  
 337 As described in the Methods 2.2, we combined images from three Landsat satellites with different sensors. Although  
 338 combining data from different sensors can lead to uncertainty in the signals (Shin et al., 2023), our result or historical  
 339 variation in the NDVI reflected the change in the forest condition observed *in situ*.

## 340 4.2 Trends in NDVI of the transect and 10-km plot

341 The NDVI of the 10-km plot showed a trend similar to that of the transect NDVI during the observation period ( $r = 0.78, p <$   
 342 0.001), as shown in Fig. 2a, and the mean NDVI value of the 10-km plot was lower than that of the transect in most years.  
 343 We found year-to-year variations in both NDVI datasets, but no significant increasing or decreasing trends were observed,

344 which is consistent with the observations during previous studies at this site (Nagano et al., 2022; Tei et al., 2019b; Lloyd et  
345 al., 2011). Therefore, our observational data can be used for the analyses of ecosystem changes not only at the plot scale but  
346 also at the regional scale.

347 **4.3 Historical variation in NDVI of typical forest**

348 We studied historical variations in NDVI and field-observed ecosystem and climatic parameters of a typical forest to  
349 understand forest conditions.

350 **4.3.1 Water availability**

351 As described in the Sect. 3.3.3, SWE controls forest NDVI because the observation site (northeastern taiga) is established in  
352 a continental dry area. We found positive and negative correlations between the NDVI and SWE. Before 2007, the TF NDVI  
353 was positively correlated with the June SWE in the current year (Fig. 4b) and positively correlated with the SWE in the  
354 previous year June, July, August, and the previous year summer (JJA: June–July–August) (Fig. 4c, 4d, S4c, and S4d, Table  
355 S5). This indicates the influence of hydrological conditions in the previous year and early summer of the current year on the  
356 leaf productivity of larch trees in the current year.

357 Larches, as deciduous trees, assimilate carbon through photosynthesis (photoassimilate) during the summer to prepare  
358 needles in the next year, and the elongation of needles may be affected by hydrological conditions in the early summer. In the  
359 Spasskaya Pad Forest, pulse-labeling experiments with  $^{13}\text{CO}_2$  showed that stored carbon from the previous year contributed  
360 approximately 50 % to formation of new needles in *Larix gmelini* saplings (Kagawa et al., 2006). The high level of water  
361 availability in the summers of 1999 and 2000 likely contributed to increased carbon storage and, as a result, the high  
362 formation of needles in 2000 and 2001. The significant NDVI decrease in 2002 was probably caused by a low level of soil  
363 moisture (i.e., dry conditions). The high summer air temperature (Fig. 2c) and the small amount of precipitation (Fig. 2d) in  
364 2001 and 2002 caused droughts in 2002 and 2003. Subsequently, the soil moisture increased due to a large amount of water  
365 year precipitation (Fig. 2d), which likely contributed to an increase in NDVI until 2007.

366 It is known that the NDVI depends on the previous-year precipitation in arid and semi-arid regions (e.g., Burry et al., 2018;  
367 Camberlin et al., 2007). In addition, historical time series of climate indices, based on both precipitation and temperature,  
368 were related to one-year lagged NDVI (e.g., Verbyla, 2015; Liu et al., 2017). In boreal interior Alaska, the summer moisture  
369 index showed a correlation with maximum summer NDVI not only at a one-year time lag in two 10-km climate station  
370 buffers but also at a two-year time lag in many other ones (Verbyla, 2015). Possible reasons for the multi-year NDVI lag  
371 could be the long-term negative vegetation responses to drought events, such as a decrease in carbon allocation by plants  
372 (e.g., Kannenberg et al., 2019) and plant mortality (e.g., Anderegg et al., 2012). Negative effects of drought events also  
373 occurred in our study.

374 As described above, the positive correlations between the TF NDVI and soil moisture were observed during 1999–2006;  
375 however, the correlations were shifted to negative values during 2008–2019 (Fig. 4b–d and S4a–e). After 2007, the TF NDVI  
376 was negatively correlated with the SWE of all months in the previous (with a one-year time lag) and current years (without a  
377 lag) (Table S6). This may indicate that after the extreme wet event, the soil moisture in the previous and current years seemed  
378 to negatively affect the current TF NDVI. Therefore, a high level of soil moisture may affect needle production (i.e., carbon  
379 assimilation, needle formation, and/or needle elongation).

380 Additionally, the  $\delta^{13}\text{C}$  values of needles at our study site often depend on water availability (Kagawa et al., 2003; Tei et al.,  
381 2019a). As shown in Fig. 5, there was the significant negative correlation between foliar  $\delta^{13}\text{C}$  and the previous August SWE  
382 in 1999–2007 ( $r = -0.79$ ,  $p < 0.05$ ). Interestingly, not only before the wet event but also for the whole observation period  
383 (1999–2019), a negative correlation was found between foliar  $\delta^{13}\text{C}$  and the previous August SWE (Fig. 5). These results  
384 differed from the correlations between the NDVI and SWE, which changed from positive to negative values. Before the wet  
385 event, under drought stress during 2001–2002, needle stomatal conductance was decreased, resulting in decreased carbon  
386 assimilation. In the subsequent years, 2002–2003, larches probably produced fewer needles (lower NDVI) with higher  $\delta^{13}\text{C}$   
387 from the previously photosynthesized C (Fig. 3a and 3d).

388 After the wet event, the foliar  $\delta^{13}\text{C}$  and SWE remained negative, indicating high stomatal conductance (low foliar  $\delta^{13}\text{C}$ ). High  
389 stomatal conductance typically contributes to the higher potential of a plant to assimilate  $\text{CO}_2$ , store C, and produce needles  
390 (high TF NDVI); however, after the wet period, larch produced fewer needles (low TF NDVI).

391 Compared with the decrease in the TF NDVI for drought events, that for the extreme wet event was smaller (Fig. 2b and 3a),  
392 although the extreme wet event caused a significant decrease in the NDVI of RF-1 and RF-2. The decrease in the TF NDVI  
393 in wet years may be due to different factors, such as nitrogen availability for larches, which can control needle formation.  
394 This factor will be discussed in the next chapter.

### 395 4.3.2 Nitrogen availability

396 Before 2007, the TF NDVI showed a significant negative correlation with foliar C/N (Fig. 4f), indicating a positive  
397 correlation with foliar N content. In this ecosystem, there have been no previous studies on the temporal correlation between  
398 NDVI and plant N content (or  $\delta^{15}\text{N}$ ). Changes in leaf nitrogen, which is an important element of chlorophyll (green pigment),  
399 were detected using NDVI (Gamon et al., 1995). Previously, the relationship between NDVI and leaf N content was  
400 predominantly investigated in crops for agricultural purposes but not in natural ecosystems. In coniferous forests, the  
401 estimation of foliar nitrogen using remote-sensing methods showed the highest uncertainty due to the complex structure of  
402 needleleaf canopies (reviewed by Homolova et al., 2013).

403 As leaf N content is considered to be an indicator of nitrogen availability for a plant in some boreal regions, where the  
404 ecosystem is usually poor in N (Matsushima et al., 2012; Liang et al., 2014), we concluded that forest greenness (NDVI) was

405 strongly controlled by nitrogen uptake by larch trees. Therefore, soil moisture is suggested to play a crucial role in  
406 maintaining forest nitrogen status. During 2000–2001, soil water was available for plants and induced favorable conditions  
407 for soil nitrogen uptake by trees. Under suitable soil moisture conditions, the production of soil inorganic N may increase.  
408 This may lead to a high production of larch needles (high NDVI). During 2002–2003—the drought years—dry conditions  
409 caused less productivity of soil inorganic N and less N uptake by trees. In the post-drought period of 2004–2007, an increase  
410 in soil moisture gradually recovered the forest conditions in terms of nitrogen uptake and needle production.

411 After 2007, the foliar C/N still showed a negative correlation with the TF NDVI during 2008–2018, but this correlation was  
412 statistically weaker compared to that during 1999–2006 (Fig. 4f). At the same time, the positive correlations between the TF  
413 NDVI and SWE changed to negative ones during 2008–2019. According to these results, high soil moisture could lead to low  
414 needle production under low nitrogen availability. When extremely high soil moisture, resulting in the saturation of soil with  
415 water, caused less production of soil inorganic nitrogen, low TF NDVI and high C/N values may be observed; thus, TF NDVI  
416 and SWE were negatively correlated.

417 While N content reflects the plant's nitrogen status, plant  $\delta^{15}\text{N}$  is widely accepted to depend on the isotopic composition of  
418 nitrogen sources (e.g., Evans, 2001). Therefore, the  $\delta^{15}\text{N}$  of soil inorganic ammonium  $\text{NH}_4^+$ , which is the main nitrogen  
419 source in the Spasskaya Pad forest (Popova et al., 2013), presumably determined the foliar  $\delta^{15}\text{N}$  in larches. As shown in Fig.  
420 3e, foliar  $\delta^{15}\text{N}$  gradually decreased after 2005. These data suggest that larch trees used less soil inorganic N, especially from  
421 the deeper soil layers, which usually have higher soil  $\delta^{15}\text{N}$  (Amundson et al., 2003; Fujiyoshi et al., 2017). This may be  
422 related to either a change in soil N dynamics, a decrease in the vertical distribution of roots (Takenaka et al., 2016), or  
423 damage to the lower roots due to extremely high soil moisture. Under root oxygen stress due to soil flooding, plant  
424 metabolism changes from aerobic respiration to anaerobic fermentation, characterized by energy deficiency and ethanol  
425 production, both of which induce decreased nutrient uptake and plant growth (reviewed by Pezeshki and Delaune, 2012).  
426 Reduced soil conditions can also induce soil phytotoxin production, damaging the root system (Pezeshki, 2001).

427 It should be noted that not only the extreme wet event in 2007, but also the extreme drought in 2001 may have caused a  
428 change in N availability. Many studies have shown that foliar  $\delta^{15}\text{N}$  increases during drought (Penuelas et al., 2000; Handley  
429 et al., 1999; Lopes and Araus, 2006; Ogaya and Penuelas, 2008). However, in the present study, the drought in 2001 and  
430 2002 decreased foliar  $\delta^{15}\text{N}$ . We could not identify the exact reason, but drought in 2001 and 2002 might have affected the N  
431 availability for larch trees.

#### 432 4.3.3 NDVI and RWI of larch trees

433 Two parameters of aboveground biomass, the RWI and TF NDVI, were positively correlated at a significant level ( $r = 0.76, p$   
434  $< 0.05$ ; Fig. 4a) during 1999–2006. Similarly, in other northern regions, temporal patterns of the NDVI and  
435 dendrochronological data were similar for larch (Erasmi et al., 2021; Berner et al., 2011; Berner et al., 2013), pine (Berner et

436 al., 2011), and spruce (Andreu-Hayles et al., 2011; Beck et al., 2013; Berner et al., 2011; Lopatin et al., 2006). This means  
437 that tree growth (RWI) and needle production (NDVI as an indicator of LAI) showed synchronous responses to  
438 environmental changes before 2007. However, there was no significant correlation between the TF NDVI and RWI after  
439 2007. Thus, the extreme wet event in 2007 could have changed the physiological response of larch trees to the environment  
440 in terms of needle and wood production.

441 The correlation between NDVI and RWI at our observation site was previously reported by Tei et al. (2019b). They used  
442 GIMMS-NDVI3g and found its positive correlation with the RWI in the subsequent year during 2004–2014 at the study site.  
443 These two parameters, the NDVI and RWI, reflect the carry-over of carbon, which is fixed via needles in the previous year  
444 and used in the current year, as experimentally demonstrated by Kagawa et al. (2006). In previous studies,  
445 dendrochronological data showed that tree growth responded to climate with a time lag (e.g., Tei and Sugimoto, 2018). In our  
446 study, we did not observe a significant correlation between the TF NDVI and RWI at the one-year lag of RWI (Fig. S4g).

#### 447 **4.4 Changes in larch forest NDVI due to drought and the extreme wet event**

448 As shown in Fig. 2b, the NDVI in TF showed a significant decrease in 2002. Such a decrease in NDVI has been repeated in  
449 the past because the climate is continental (dry) in this region. Compared to this decrease in NDVI due to drought, the  
450 extreme wet event in 2007 showed only a slight decrease in the NDVI in TF, although the NDVI in DF and RF-2 decreased  
451 considerably.

452 Tree mortality in the DF and RF during the extreme wet event is controlled by soil properties and topographic features, that  
453 is, depressions (Iwasaki et al., 2010). However, the effects of the event may not only include tree mortality but also invisible  
454 damage to living trees. In this study, NDVI, a potential indicator of needle production in a typical forest, was negatively  
455 related to the summer SWE in the previous and current years during 2008–2019 and with the current-year needle C/N during  
456 2008–2018 (Table S6). This may indicate that needle production in the current and subsequent years during the summer was  
457 disturbed by increased soil moisture and decreased soil N uptake by trees. We suggest that N uptake by larches might be  
458 reduced in wet soils due to damaged lower roots, decreased vertical distribution of roots (Takenaka et al., 2016), or altered  
459 soil N production.

460 Changes in the process of needle production may affect tree growth in the current and subsequent years in the forest (Kagawa  
461 et al., 2006; Tei et al., 2019b). However, we found no evidence that tree radial growth was disturbed after 2007, and the RWI  
462 responded well to changes in the SWE (Fig. 3b and 3c). Additionally, at the ecosystem scale, there was no significant change  
463 in the CO<sub>2</sub> exchange measured by the 32-m flux tower in this larch forest (Kotani et al., 2019). However, the observed  
464 increase in understory biomass was suggested to compensate for negative changes in fluxes at the overstory level (Kotani et  
465 al., 2019) and in the NDVI of the forest (Nagano et al., 2022). This means that the negative effects of the extreme wet event  
466 on living larch trees were not excluded in the previous studies. Our study showed that limitation in N uptake at high soil

467 moisture levels is one of the factors that may potentially reduce tree growth in the future.  
468 In our previous study (Nogovitcyn et al., 2022), spatial variations in NDVI and foliar traits identified favorable conditions in  
469 the sites affected by the extreme wet event (RF). The larch forest in RF with lower NDVI (lower stand density) had higher  
470 light (higher  $\delta^{13}\text{C}$ ) and nitrogen (lower foliar C/N) availability for one mature larch tree than that in unaffected areas (TF)  
471 because of reduced competition for light and soil nitrogen among trees. Such favorable conditions and the presence of a large  
472 number of young larch trees may lead to further RF succession after an extremely wet event. However, because weather  
473 extremes are expected to be more frequent and intensive (Douville et al., 2021), the period between extremes may exceed the  
474 period of recovery after the extremes. Therefore, in the future, forests may be damaged rather than recovered.

475 We showed that NDVI values in affected areas were lower than those in typical larch forests for more than 10 years after the  
476 extreme wet event. In other boreal regions, the NDVI was higher in damaged forests because of the strong contribution of  
477 understory to surface greenness (Bunn et al., 2007; Dearborn and Baltzer, 2021), suggesting the need to combine field and  
478 remote sensing observations. Regarding the prediction of tree growth in this dry region, there is a discrepancy between the  
479 different vegetation models. The dynamic global vegetation model (DGVM) simulated increased forest production  
480 throughout the circumboreal region in the nearest century, whereas the RWI-based model showed the opposite result in the  
481 regions of Alaska, Canada, Europe and our study site (Tei et al., 2017). In these regions with a continentally dry climate, tree  
482 growths suffers because of the effects of temperature-induced drought stress and are predicted to decrease under warming  
483 conditions (Tei et al., 2017). In addition, extreme wet events are also likely to have a negative impact on forest production  
484 because of changes in nitrogen availability, as demonstrated in this study. Some models may overestimate production  
485 because they do not include important parameters such as soil moisture, soil N production, and N uptake by trees. To better  
486 understand changes in the forest, long-term observation of variations in soil N availability depending on soil moisture and  
487 other factors is necessary.

## 488 5 Conclusions

489 In this study, historical variations in satellite-derived NDVI (seasonal maximum) and field-observed parameters of larch  
490 forests were investigated to understand the effects of the extreme wet event on the larch forests of northeastern Siberia. The  
491 NDVI values of the plots visually unaffected (typical mature larch forest, TF) and affected by the event were similar before  
492 2007, and the NDVI values at both plots were similarly decreased by drought. However, both NDVI values ~~but~~ differed after  
493 2007 because of the high tree mortality in affected plots caused by waterlogging and the presence of water in the depression.  
494 Although the TF was visually unaffected by the event, it also changed. Before the wet event, the positive relationship  
495 between the TF NDVI and SWE in the previous summer and the current June showed that needle production increased with  
496 water availability, as previously observed in this dry region. However, after the wet event, the relationship between the TF

497 NDVI and soil moisture in the previous and current years unexpectedly shifted from positive to negative, which may have  
498 been related to N availability.

499 N is considered an important factor controlling needle production before and after the wet event, as the negative correlations  
500 between TF NDVI and needle C/N ratio were observed until 2018 (except for in 2007). In addition, the needle  $\delta^{15}\text{N}$   
501 continuously decreased after the wet event, suggesting that the larch trees used a different N source when the lower roots  
502 were damaged by anaerobic conditions. Before the wet event, the high (but suitable) soil moisture level presumably produced  
503 more soil inorganic N, and consequently produced more larch needles, whereas the extreme wetness after 2007 likely had a  
504 long-term negative effect on needle production because of the lower soil N production. As shown in this study, extreme wet  
505 events in continental dry regions may alter the interaction between water availability and tree performance (for example,  
506 NDVI) over a long time because of shifts in N availability for trees.

507 **Data availability.** Yakutsk air temperature and precipitation data are available from the RIHMI-WDC website (<http://aisori-m.meteo.ru/>). NDVI data was calculated from Landsat 5, 7, 8 images, which are available from the USGS website  
508 (<https://earthexplorer.usgs.gov/>). The seasonal maximum NDVI data and larch RWI data are described in the Supplement  
509 (Table S1 and S2). All other data presented in this work have been deposited in the Arctic Data Archive System (ADS): soil  
510 moisture data at Spasskaya Pad (<https://ads.nipr.ac.jp/dataset/A20230217-001>) and larch needle C/N and carbon and nitrogen  
511 isotopes at Spasskaya Pad (<https://ads.nipr.ac.jp/dataset/A20230217-002>).  
512

513 **Author contributions.** AS designed the research and AN calculated the NDVI and performed the analyses. TM, ST, and NS  
514 helped with the analyses, and TCM managed all the field observations. RS and YM helped with field observations. AN and  
515 AS prepared the paper with contributions from all co-authors.

516 **Competing interests.** The authors declare that they have no conflict of interest.

517 **Acknowledgements.** The authors are grateful to Dr. A. Kononov, R. Petrov, and other colleagues from the IBPC for  
518 supporting our fieldwork at the Spasskaya Pad Forest Station and M. Grigorev for his assistance in the fieldwork. The  
519 authors also appreciate Y. Hoshino, S. Nunohashi, A. Alekseeva, and E. Starostin for their support in laboratory work and  
520 logistics.

521 **Financial support.** This work was supported by the Belmont Forum Arctic program COPERA (C budget of ecosystems,  
522 cities, and villages on permafrost in the eastern Russian Arctic) project, the International Priority Graduate Programs (IPGP),  
523 funded by the Ministry of Education, Culture, Sports, Science, and Technology-Japan (MEXT), and the Hokkaido University  
524 DX Doctoral Fellowship (Grant No. JPMJSP2119), funded by the Japan Science and Technology Agency.

525 **References**

526 Abaimov, A. P., Lesinski, J. A., Martinsson, O., and Milyutin, L. I.: Variability and ecology of Siberian larch species,  
527 Swedish University of Agricultural Sciences. Departament of Silviculture. Reports., Umeå, 123 pp., 1998.

528 Amundson, R., Austin, A. T., Schuur, E. A. G., Yoo, K., Matzek, V., Kendall, C., Uebersax, A., Brenner, D., and Baisden, W.  
529 T.: Global patterns of the isotopic composition of soil and plant nitrogen, *Global Biogeochemical Cycles*, 17,  
530 10.1029/2002gb001903, 2003.

531 Anderegg, W. R. L., Berry, J. A., Smith, D. D., Sperry, J. S., Anderegg, L. D. L., and Field, C. B.: The roles of hydraulic and  
532 carbon stress in a widespread climate-induced forest die-off, *Proceedings of the National Academy of Sciences of the United  
533 States of America*, 109, 233-237, 10.1073/pnas.1107891109, 2012.

534 Andreu-Hayles, L., D'Arrigo, R., Anchukaitis, K. J., Beck, P. S. A., Frank, D., and Goetz, S.: Varying boreal forest response  
535 to Arctic environmental change at the Firth River, Alaska, *Environmental Research Letters*, 6, 10.1088/1748-  
536 9326/6/4/045503, 2011.

537 Archibald, O. W.: The coniferous forests, in: *Ecology of World Vegetation*, 238–279, 10.1007/978-94-011-0009-0\_8 1995.

538 Beck, P. S. A., Andreu-Hayles, L., D'Arrigo, R., Anchukaitis, K. J., Tucker, C. J., Pinzon, J. E., and Goetz, S. J.: A large-scale  
539 coherent signal of canopy status in maximum latewood density of tree rings at arctic treeline in North America, *Global and  
540 Planetary Change*, 100, 109-118, 10.1016/j.gloplacha.2012.10.005, 2013.

541 Berner, L. T., Beck, P. S. A., Bunn, A. G., and Goetz, S. J.: Plant response to climate change along the forest-tundra ecotone  
542 in northeastern Siberia, *Global Change Biology*, 19, 3449-3462, 10.1111/gcb.12304, 2013.

543 Berner, L. T., Beck, P. S. A., Bunn, A. G., Lloyd, A. H., and Goetz, S. J.: High-latitude tree growth and satellite vegetation  
544 indices: Correlations and trends in Russia and Canada (1982-2008), *Journal of Geophysical Research-Biogeosciences*, 116,  
545 10.1029/2010jg001475, 2011.

546 Bunn, A. G. and Goetz, S. J.: Trends in satellite-observed circumpolar photosynthetic activity from 1982 to 2003: The  
547 influence of seasonality, cover type, and vegetation density, *Earth Interactions*, 10, 2006.

548 Bunn, A. G., Goetz, S. J., Kimball, J. S., and Zhang, K.: Northern high-latitude ecosystems respond to climate change,  
549 10.1029/2007EO340001, 2007.

550 Burry, L. S., Palacio, P. I., Somoza, M., de Mandri, M. E. T., Lindsoug, H. B., Marconetto, M. B., and D'Antoni, H. L.:  
551 Dynamics of fire, precipitation, vegetation and NDVI in dry forest environments in NW Argentina. Contributions to  
552 environmental archaeology, *Journal of Archaeological Science-Reports*, 18, 747-757, 10.1016/j.jasrep.2017.05.019, 2018.

553 Camberlin, P., Martiny, N., Philippon, N., and Richard, Y.: Determinants of the interannual relationships between remote  
554 sensed photosynthetic activity and rainfall in tropical Africa, *Remote Sensing of Environment*, 106, 199-216,  
555 10.1016/j.rse.2006.08.009, 2007.

556 Dearborn, K. D. and Baltzer, J. L.: Unexpected greening in a boreal permafrost peatland undergoing forest loss is partially  
557 attributable to tree species turnover, *Global Change Biology*, 27, 2867-2882, 10.1111/gcb.15608, 2021.

558 Douville, H., Raghavan, K., Renwick, J., Allan, R. P., Arias, P. A., Barlow, M., Cerezo-Mota, R., Cherchi, A., Gan, T. Y.,  
559 Gergis, J., Jiang, D., Khan, A., Pokam Mba, W., Rosenfeld, D., Tierney, J., and Zolina, O.: Water Cycle Changes, in: *Climate  
560 Change 2021: The Physical Science Basis. Contribution of Working Group I to the Sixth Assessment Report of the*

561 Intergovernmental Panel on Climate Change edited by: Masson-Delmotte, V., Zhai, P., Pirani, A., Connors, S. L., Péan, C.,  
562 Berger, S., Caud, N., Chen, Y., Goldfarb, L., Gomis, M. I., Huang, M., Leitzell, K., Lonnoy, E., Matthews, J. B. R., Maycock,  
563 T. K., Waterfield, T., Yelekçi, O., Yu, R., and Zhou, B., Cambridge University Press, Cambridge, United Kingdom and New  
564 York 1055–1210, 10.1017/9781009157896.010.—, 2021.

565 Erasmi, S., Klinge, M., Dulamsuren, C., Schneider, F., and Hauck, M.: Modelling the productivity of Siberian larch forests  
566 from Landsat NDVI time series in fragmented forest stands of the Mongolian forest-steppe, *Environmental Monitoring and*  
567 *Assessment*, 193, 10.1007/s10661-021-08996-1, 2021.

568 Evans, R. D.: Physiological mechanisms influencing plant nitrogen isotope composition, *Trends in Plant Science*, 6, 121-126,  
569 10.1016/s1360-1385(01)01889-1, 2001.

570 Famiglietti, C. A., Michalak, A. M., and Konings, A. G.: Extreme wet events as important as extreme dry events in  
571 controlling spatial patterns of vegetation greenness anomalies, *Environmental Research Letters*, 16, 10.1088/1748-  
572 9326/abfc78, 2021.

573 Fan, R., Shimada, H., Tei, S., Maximov, T. C., and Sugimoto, A.: Oxygen Isotope Compositions of Cellulose in Earlywood of  
574 Larix cajanderi Determined by Water Source Rather Than Leaf Water Enrichment in a Permafrost Ecosystem, Eastern  
575 Siberia, *Journal of Geophysical Research-Biogeosciences*, 126, 10.1029/2020jg006125, 2021.

576 FAO: Global Forest Resources Assessment 2020 – Key findings, Rome, 10.4060/ca8753en, 2020.

577 Farquhar, G. D., Ehleringer, J. R., and Hubick, K. T.: Carbon isotope discrimination and photosynthesis, *Annual Review of*  
578 *Plant Physiology and Plant Molecular Biology*, 40, 503-537, 10.1146/annurev.pp.40.060189.002443, 1989.

579 Forbes, B. C., Fauria, M. M., and Zetterberg, P.: Russian Arctic warming and 'greening' are closely tracked by tundra shrub  
580 willows, *Global Change Biology*, 16, 1542-1554, 10.1111/j.1365-2486.2009.02047.x, 2010.

581 Forkel, M., Migliavacca, M., Thonicke, K., Reichstein, M., Schaphoff, S., Weber, U., and Carvalhais, N.: Codominant water  
582 control on global interannual variability and trends in land surface phenology and greenness, *Global Change Biology*, 21,  
583 3414-3435, 10.1111/gcb.12950, 2015.

584 Friedlingstein, P., Jones, M. W., O'Sullivan, M., Andrew, R. M., Bakker, D. C. E., Hauck, J., Le Quere, C., Peters, G. P.,  
585 Peters, W., Pongratz, J., Sitch, S., Canadell, J. G., Ciais, P., Jackson, R. B., Alin, S. R., Anthoni, P., Bates, N. R., Becker, M.,  
586 Bellouin, N., Bopp, L., Chau, T. T. T., Chevallier, F., Chini, L. P., Cronin, M., Currie, K. I., Decharme, B., Djeutchouang, L.,  
587 Dou, X. Y., Evans, W., Feely, R. A., Feng, L., Gasser, T., Gilfillan, D., Gkritzalis, T., Grassi, G., Gregor, L., Gruber, N.,  
588 Gurses, O., Harris, I., Houghton, R. A., Hurtt, G. C., Iida, Y., Ilyina, T., Luijkx, I. T., Jain, A., Jones, S. D., Kato, E., Kennedy,  
589 D., Goldewijk, K. K., Knauer, J., Korsbakken, J. I., Kortzinger, A., Landschutze, P., Lauvset, S. K., Lefevre, N., Lienert, S.,  
590 Liu, J. J., Marland, G., McGuire, P. C., Melton, J. R., Munro, D. R., Nabel, J., Nakaoka, S. I., Niwa, Y., Ono, T., Pierrot, D.,  
591 Poulter, B., Rehder, G., Resplandy, L., Robertson, E., Rodenbeck, C., Rosan, T. M., Schwinger, J., Schwingshakl, C.,  
592 Seferian, R., Sutton, A. J., Sweeney, C., Tanhua, T., Tans, P. P., Tian, H. Q., Tilbrook, B., Tubiello, F., van der Werf, G. R.,  
593 Vuichard, N., Wada, C., Wanninkhof, R., Watson, A. J., Willis, D., Wiltshire, A. J., Yuan, W. P., Yue, C., Yue, X., Zaehle, S.,  
594 and Zeng, J. Y.: Global Carbon Budget 2021, *Earth System Science Data*, 14, 1917-2005, 10.5194/essd-14-1917-2022, 2022.

595 Frost, G. V. and Epstein, H. E.: Tall shrub and tree expansion in Siberian tundra ecotones since the 1960s, *Global Change*  
596 *Biology*, 20, 1264-1277, 10.1111/gcb.12406, 2014.

597 Fujiyoshi, L., Sugimoto, A., Tsukuura, A., Kitayama, A., Caceres, M. L. L., Mijidsuren, B., Saraadanbazar, A., and  
598 Tsujimura, M.: Spatial variations in larch needle and soil N-15 at a forest-grassland boundary in northern Mongolia, *Isotopes*  
599 in Environmental and Health Studies

600 Gamon, J. A., Field, C. B., Goulden, M. L., Griffin, K. L., Hartley, A. E., Joel, G., Penuelas, J., and Valentini, R.:  
601 Relationships between NDVI, canopy structure, and photosynthesis in 3 Californian vegetation types, *Ecological*  
602 *Applications*, 5, 28-41, 10.2307/1942049, 1995.

603 Goetz, S. J., Bunn, A. G., Fiske, G. J., and Houghton, R. A.: Satellite-observed photosynthetic trends across boreal North  
604 America associated with climate and fire disturbance, *Proceedings of the National Academy of Sciences of the United States*  
605 of America

606 Handley, L. L., Azcon, R., Lozano, J. M. R., and Scrimgeour, C. M.: Plant delta N-15 associated with arbuscular  
607 mycorrhization, drought and nitrogen deficiency, *Rapid Communications in Mass Spectrometry*, 13, 1320-1324, 1999.

608 Holben, B. N.: Characteristics of maximum-value composite images from temporal AVHRR data, *International Journal of*  
609 *Remote Sensing*, 7, 1417-1434, 10.1080/01431168608948945, 1986.

610 Homolova, L., Maenovsky, Z., Clevers, J., Garcia-Santos, G., and Schaeprnan, M. E.: Review of optical-based remote  
611 sensing for plant trait mapping, *Ecological Complexity*, 15, 1-16, 10.1016/j.ecocom.2013.06.003, 2013.

612 Huete, A., Didan, K., Miura, T., Rodriguez, E. P., Gao, X., and Ferreira, L. G.: Overview of the radiometric and biophysical  
613 performance of the MODIS vegetation indices, *Remote Sensing of Environment*, 83, 195-213, 10.1016/s0034-  
614 4257(02)00096-2, 2002.

615 Iijima, Y., Ohta, T., Kotani, A., Fedorov, A. N., Kodama, Y., and Maximov, T. C.: Sap flow changes in relation to permafrost  
616 degradation under increasing precipitation in an eastern Siberian larch forest, *Ecohydrology*, 7, 177-187, 10.1002/eco.1366,  
617 2014.

618 Iwasaki, H., Saito, H., Kuwao, K., Maximov, T. C., and Hasegawa, S.: Forest decline caused by high soil water conditions in  
619 a permafrost region, *Hydrology and Earth System Sciences*, 14, 301-307, 10.5194/hess-14-301-2010, 2010.

620 Ju, J. C. and Masek, J. G.: The vegetation greenness trend in Canada and US Alaska from 1984-2012 Landsat data, *Remote*  
621 *Sensing of Environment*, 176, 1-16, 10.1016/j.rse.2016.01.001, 2016.

622 Kagawa, A., Sugimoto, A., and Maximov, T. C.: Seasonal course of translocation, storage and remobilization of C-13 pulse-  
623 labeled photoassimilate in naturally growing *Larix gmelinii* saplings, *New Phytologist*, 171, 793-804, 10.1111/j.1469-  
624 8137.2006.01780.x, 2006.

625 Kagawa, A., Naito, D., Sugimoto, A., and Maximov, T. C.: Effects of spatial and temporal variability in soil moisture on  
626 widths and delta C-13 values of eastern Siberian tree rings, *Journal of Geophysical Research-Atmospheres*, 108,  
627 10.1029/2002jd003019, 2003.

628 Kajimoto, T., Matsuura, Y., Sofronov, M. A., Volokitina, A. V., Mori, S., Osawa, A., and Abaimov, A. P.: Above- and  
629 belowground biomass and net primary productivity of a *Larix gmelinii* stand near Tura, central Siberia, *Tree Physiology*, 19,  
630 815-822, 1999.

631 Kannenberg, S. A., Novick, K. A., Alexander, M. R., Maxwell, J. T., Moore, D. J. P., Phillips, R. P., and Anderegg, W. R. L.:  
632 Linking drought legacy effects across scales: From leaves to tree rings to ecosystems, *Global Change Biology*, 25, 2978-

633 2992, 10.1111/gcb.14710, 2019.

634 Kotani, A., Saito, A., Kononov, A. V., Petrov, R. E., Maximov, T. C., Iijima, Y., and Ohta, T.: Impact of unusually wet  
635 permafrost soil on understory vegetation and CO<sub>2</sub> exchange in a larch forest in eastern Siberia, Agricultural and Forest  
636 Meteorology, 265, 295-309, 10.1016/j.agrformet.2018.11.025, 2019.

637 Liang, M. C., Sugimoto, A., Tei, S., Bragin, I. V., Takano, S., Morozumi, T., Shingubara, R., Maximov, T. C., Kiyashko, S. I.,  
638 Velivetskaya, T. A., and Ignatiev, A. V.: Importance of soil moisture and N availability to larch growth and distribution in the  
639 Arctic taiga-tundra boundary ecosystem, northeastern Siberia, Polar Science, 8, 327-341, 10.1016/j.polar.2014.07.008, 2014.

640 Liu, J. X., Price, D. T., and Chen, J. A.: Nitrogen controls on ecosystem carbon sequestration: a model implementation and  
641 application to Saskatchewan, Canada, Ecological Modelling, 186, 178-195, 10.1016/j.ecolmodel.2005.01.036, 2005.

642 Liu, S. L., Zhang, Y. Q., Cheng, F. Y., Hou, X. Y., and Zhao, S.: Response of Grassland Degradation to Drought at Different  
643 Time-Scales in Qinghai Province: Spatio-Temporal Characteristics, Correlation, and Implications, Remote Sensing, 9,  
644 10.3390/rs9121329, 2017.

645 Lloyd, A. H., Bunn, A. G., and Berner, L.: A latitudinal gradient in tree growth response to climate warming in the Siberian  
646 taiga, Global Change Biology, 17, 1935-1945, 10.1111/j.1365-2486.2010.02360.x, 2011.

647 Lopatin, E., Kolstrom, T., and Spiecker, H.: Determination of forest growth trends in Komi Republic (northwestern Russia):  
648 combination of tree-ring analysis and remote sensing data, Boreal Environment Research, 11, 341-353, 2006.

649 Lopes, M. S. and Araus, J. L.: Nitrogen source and water regime effects on durum wheat photosynthesis and stable carbon  
650 and nitrogen isotope composition, Physiologia Plantarum, 126, 435-445, 10.1111/j.1399-3054.2006.00595.x, 2006.

651 Matsumoto, K., Ohta, T., Nakai, T., Kuwada, T., Daikoku, K., Iida, S., Yabuki, H., Kononov, A. V., van der Molen, M. K.,  
652 Kodama, Y., Maximov, T. C., Dolman, A. J., and Hattori, S.: Responses of surface conductance to forest environments in the  
653 Far East, Agricultural and Forest Meteorology, 148, 1926-1940, 10.1016/j.agrformet.2008.09.009, 2008.

654 Matsushima, M., Choi, W. J., and Chang, S. X.: White spruce foliar delta C-13 and delta N-15 indicate changed soil N  
655 availability by understory removal and N fertilization in a 13-year-old boreal plantation, Plant and Soil, 361, 375-384,  
656 10.1007/s11104-012-1254-z, 2012.

657 Miles, V. V. and Esau, I.: Spatial heterogeneity of greening and browning between and within bioclimatic zones in northern  
658 West Siberia, Environmental Research Letters, 11, 10.1088/1748-9326/11/11/115002, 2016.

659 Myers-Smith, I. H., Kerby, J. T., Phoenix, G. K., Bjerke, J. W., Epstein, H. E., Assmann, J. J., John, C., Andreu-Hayles, L.,  
660 Angers-Blondin, S., Beck, P. S. A., Berner, L. T., Bhatt, U. S., Bjorkman, A. D., Blok, D., Bryn, A., Christiansen, C. T.,  
661 Cornelissen, J. H. C., Cunliffe, A. M., Elmendorf, S. C., Forbes, B. C., Goetz, S. J., Hollister, R. D., de Jong, R., Loranty, M.  
662 M., Macias-Fauria, M., Maseyk, K., Normand, S., Olofsson, J., Parker, T. C., Parmentier, F. J. W., Post, E., Schaepman-Strub,  
663 G., Stordal, F., Sullivan, P. F., Thomas, H. J. D., Tommervik, H., Treharne, R., Tweedie, C. E., Walker, D. A., Wilming, M.,  
664 and Wipf, S.: Complexity revealed in the greening of the Arctic, Nature Climate Change, 10, 106-117, 10.1038/s41558-019-  
665 0688-1, 2020.

666 Nagano, H., Kotani, A., Mizuuchi, H., Ichii, K., Kanamori, H., and Hiyama, T.: Contrasting 20-year trends in NDVI at two  
667 Siberian larch forests with and without multiyear waterlogging-induced disturbances, Environmental Research Letters, 17,  
668 10.1088/1748-9326/ac4884, 2022.

669 Nakai, T., Hiyama, T., Petrov, R. E., Kotani, A., Ohta, T., and Maximov, T. C.: Application of an open-path eddy covariance  
670 methane flux measurement system to a larch forest in eastern Siberia, *Agricultural and Forest Meteorology*, 282,  
671 10.1016/j.agrformet.2019.107860, 2020.

672 Nogovitcyn, A., Shakhmatov, R., Morozumi, T., Tei, S., Miyamoto, Y., Shin, N., Maximov, T. C., and Sugimoto, A.: Changes  
673 in Forest Conditions in a Siberian Larch Forest Induced by an Extreme Wet Event, *Forests*, 13, 10.3390/f13081331, 2022.

674 Ogaya, R. and Penuelas, J.: Changes in leaf delta C-13 and delta N-15 for three Mediterranean tree species in relation to soil  
675 water availability, *Acta Oecologica-International Journal of Ecology*, 34, 331-338, 10.1016/j.actao.2008.06.005, 2008.

676 Ohta, T., Kotani, A., Iijima, Y., Maximov, T. C., Ito, S., Hanamura, M., Kononov, A. V., and Maximov, A. P.: Effects of  
677 waterlogging on water and carbon dioxide fluxes and environmental variables in a Siberian larch forest, 1998-2011,  
678 *Agricultural and Forest Meteorology*, 188, 64-75, 10.1016/j.agrformet.2013.12.012, 2014.

679 Penuelas, J., Filella, I., Lloret, F., Pinol, J., and Siscart, D.: Effects of a severe drought on water and nitrogen use by *Quercus*  
680 *ilex* and *Phillyrea latifolia*, *Biologia Plantarum*, 43, 47-53, 10.1023/a:1026546828466, 2000.

681 Pezeshki, S. R.: Wetland plant responses to soil flooding, *Environmental and Experimental Botany*, 46, 299-312,  
682 10.1016/s0098-8472(01)00107-1, 2001.

683 Pezeshki, S. R. and DeLaune, R. D.: Soil Oxidation-Reduction in Wetlands and Its Impact on Plant Functioning,  
684 10.3390/biology1020196, 2012.

685 Popova, A. S., Tokuchi, N., Ohte, N., Ueda, M. U., Osaka, K., Maximov, T. C., and Sugimoto, A.: Nitrogen availability in the  
686 taiga forest ecosystem of northeastern Siberia, *Soil Science and Plant Nutrition*, 59, 427-441,  
687 10.1080/00380768.2013.772495, 2013.

688 Roy, D. P., Kovalskyy, V., Zhang, H. K., Vermote, E. F., Yan, L., Kumar, S. S., and Egorov, A.: Characterization of Landsat-7  
689 to Landsat-8 reflective wavelength and normalized difference vegetation index continuity, *Remote Sensing of Environment*,  
690 185, 57-70, 10.1016/j.rse.2015.12.024, 2016.

691 Ruiz-Perez, G. and Vico, G.: Effects of Temperature and Water Availability on Northern European Boreal Forests, *Frontiers*  
692 in Forests and Global Change

693 Sato, H. and Kobayashi, H.: Topography Controls the Abundance of Siberian Larch Forest, *Journal of Geophysical Research-  
694 Biogeosciences*, 123, 106-116, 10.1002/2017jg004096, 2018.

695 Schuur, E. A. G., McGuire, A. D., Schadel, C., Grosse, G., Harden, J. W., Hayes, D. J., Hugelius, G., Koven, C. D., Kuhry, P.,  
696 Lawrence, D. M., Natali, S. M., Olefeldt, D., Romanovsky, V. E., Schaefer, K., Turetsky, M. R., Treat, C. C., and Vonk, J. E.:  
697 Climate change and the permafrost carbon feedback, *Nature*, 520, 171-179, 10.1038/nature14338, 2015.

698 Shakhmatov, R., Hashiguchi, S., Maximov, T. C., and Sugimoto, A.: Effects of snow manipulation on larch trees in the taiga  
699 forest ecosystem in northeastern Siberia, *Progress in Earth and Planetary Science*, 9, 10.1186/s40645-021-00460-5, 2022.

700 Sugimoto, A.: Stable Isotopes of Water in Permafrost Ecosystem, in: *Water-Carbon Dynamics in Eastern Siberia. Ecological*  
701 *Studies (Analysis and Synthesis)*, edited by: Ohta, T., Hiyama, T., Iijima, Y., Kotani, A., and Maximov, T., Springer,  
702 Singapore, 10.1007/978-981-13-6317-7\_6, 2019.

703 Shevtsova, I., Heim, B., Kruse, S., Schroder, J., Troeva, E. I., Pestryakova, L. A., Zakharov, E. S., and Herzschuh, U.: Strong  
704 shrub expansion in tundra-taiga, tree infilling in taiga and stable tundra in central Chukotka (north-eastern Siberia) between

705 2000 and 2017, *Environmental Research Letters*, 15, 10.1088/1748-9326/ab9059, 2020.

706 Shin, N., Saitoh, T. M., Takeuchi, Y., Miura, T., Aiba, M., Kurokawa, H., Onoda, Y., Ichii, K., Nasahara, K. N., Suzuki, R.,

707 Nakashizuka, T., and Muraoka, H.: Review: Monitoring of land cover changes and plant phenology by remote-sensing in

708 East Asia, *Ecological Research*, 38, 111-133, 10.1111/1440-1703.12371, 2023.

709 Sugimoto, A., Yanagisawa, N., Naito, D., Fujita, N., and Maximov, T. C.: Importance of permafrost as a source of water for

710 plants in east Siberian taiga, *Ecological Research*, 17, 493-503, 10.1046/j.1440-1703.2002.00506.x, 2002.

711 Sugimoto, A., Naito, D., Yanagisawa, N., Ichiyangi, K., Kurita, N., Kubota, J., Kotake, T., Ohata, T., Maximov, T. C., and

712 Fedorov, A. N.: Characteristics of soil moisture in permafrost observed in East Siberian taiga with stable isotopes of water,

713 *Hydrological Processes*, 17, 1073-1092, 10.1002/hyp.1180, 2003.

714 Takata, K., Patra, P. K., Kotani, A., Mori, J., Belikov, D., Ichii, K., Saeki, T., Ohta, T., Saito, K., Ueyama, M., Ito, A.,

715 Maksyutov, S., Miyazaki, S., Burke, E. J., Ganshin, A., Iijima, Y., Ise, T., Machiya, H., Maximov, T. C., Niwa, Y., O'Ishi, R.,

716 Park, H., Sasai, T., Sato, H., Tei, S., Zhuravlev, R., Machida, T., Sugimoto, A., and Aoki, S.: Reconciliation of top-down and

717 bottom-up CO<sub>2</sub> fluxes in Siberian larch forest, *Environmental Research Letters*, 12, 10.1088/1748-9326/aa926d, 2017.

718 Takenaka, C., Miyahara, M., Ohta, T., and Maximov, T. C.: Response of larch root development to annual changes of water

719 conditions in eastern Siberia, *Polar Science*, 10, 160-166, 10.1016/j.polar.2016.04.012, 2016.

720 Tape, K., Sturm, M., and Racine, C.: The evidence for shrub expansion in Northern Alaska and the Pan-Arctic, *Global*

721 *Change Biology*, 12, 686-702, 10.1111/j.1365-2486.2006.01128.x, 2006.

722 Tei, S. and Sugimoto, A.: Time lag and negative responses of forest greenness and tree growth to warming over circumboreal

723 forests, *Global Change Biology*, 24, 4225-4237, 10.1111/gcb.14135, 2018.

724 Tei, S., Sugimoto, A., Yonenobu, H., Kotani, A., and Maximov, T. C.: Effects of extreme drought and wet events for tree

725 mortality: Insights from tree-ring width and carbon isotope ratio in a Siberian larch forest, *Ecohydrology*, 12,

726 10.1002/eco.2143, 2019a.

727 Tei, S., Sugimoto, A., Yonenobu, H., Yamazaki, T., and Maximov, T. C.: Reconstruction of soil moisture for the past 100

728 years in eastern Siberia by using delta C-13 of larch tree rings, *Journal of Geophysical Research-Biogeosciences*, 118, 1256-

729 1265, 10.1002/jgrg.20110, 2013.

730 Tei, S., Sugimoto, A., Kotani, A., Ohta, T., Morozumi, T., Saito, S., Hashiguchi, S., and Maximov, T.: Strong and stable

731 relationships between tree-ring parameters and forest-level carbon fluxes in a Siberian larch forest, *Polar Science*, 21, 146-

732 157, 10.1016/j.polar.2019.02.001, 2019b.

733 Tei, S., Sugimoto, A., Yonenobu, H., Matsuura, Y., Osawa, A., Sato, H., Fujinuma, J., and Maximov, T.: Tree-ring analysis

734 and modeling approaches yield contrary response of circumboreal forest productivity to climate change, *Global Change*

735 *Biology*, 23, 5179-5188, 10.1111/gcb.13780, 2017.

736 Verbyla, D.: The greening and browning of Alaska based on 1982-2003 satellite data, *Global Ecology and Biogeography*, 17,

737 547-555, 10.1111/j.1466-8238.2008.00396.x, 2008.

738 Verbyla, D.: Remote sensing of interannual boreal forest NDVI in relation to climatic conditions in interior Alaska,

739 *Environmental Research Letters*, 10, 10.1088/1748-9326/10/12/125016, 2015.

740 Wang, P., Huang, Q. W., Tang, Q., Chen, X. L., Yu, J. J., Pozdniakov, S. P., and Wang, T. Y.: Increasing annual and extreme

741 precipitation in permafrost-dominated Siberia during 1959-2018, Journal of Hydrology, 603, 10.1016/j.jhydrol.2021.126865,  
742 2021.  
743 Welp, L. R., Randerson, J. T., and Liu, H. P.: The sensitivity of carbon fluxes to spring warming and summer drought  
744 depends on plant functional type in boreal forest ecosystems, Agricultural and Forest Meteorology, 147, 172-185,  
745 10.1016/j.agrformet.2007.07.010, 2007.